





# Imaging of Non-malignant Conditions of the Prostate and Seminal Vesicles: A Comprehensive Review

Anuradha Chandramohan<sup>1</sup> Antony Augustine<sup>1</sup> Aisha Lakhani<sup>1</sup> Harsha Veena Kanamathareddy<sup>1</sup> Shibangi Patnaik<sup>1</sup> Sonia Thanikaivelu<sup>1</sup> Sneha Hiriyanna<sup>1</sup> Reetu John<sup>1</sup> Betty Simon<sup>1</sup> Anu Eapen<sup>1</sup> Vikram Raj Gopinathan<sup>2</sup>

<sup>1</sup> Department of Radiology, Christian Medical College, Vellore, Tamil Nadu, India

<sup>2</sup> Department of Pathology, Christian Medical College, Vellore, Tamil Nadu, India

**Address for correspondence** Anuradha Chandramohan, MD, FRCR, Department of Radiology, Christian Medical College and Hospital, Vellore 632004, Tamil Nadu, India (e-mail: anuradhachandramohan@gmail.com).

J Gastrointestinal Abdominal Radiol ISGAR

## Abstract

Non-malignant conditions of the prostate and seminal vesicles are much more common in imaging practice than prostate cancer. They include benign prostatic hyperplasia, infective and inflammatory prostatitis, prostatic and periprostatic cysts, and benign tumors. The advances in magnetic resonance imaging (MRI) of the prostate gland have dramatically improved the ability to identify these entities, many of them being identified incidentally in patients evaluated for other indications. Good knowledge of these conditions can aid in precise diagnosis and avoid interpretation pitfalls. In this article, we present non-malignant conditions of the prostate gland using several imaging modalities, including transrectal ultrasound, MRI, and computed tomography. We also present the pathological correlation for benign tumors.

## Keywords

- ▶ benign
- ▶ prostate
- ▶ seminal vesicles
- ▶ magnetic resonance imaging
- ▶ MRI

## Introduction

Non-malignant conditions of the prostate and seminal vesicles (SVs) are common in clinical practice and often detected incidentally while reporting imaging studies. These include age-related changes such as benign prostatic hyperplasia, congenital and acquired prostatic and periprostatic cysts, infective and inflammatory changes in the prostate, and benign neoplasms. In multi-parametric MRI (mpMRI) of the prostate, many of these entities contribute significantly to pitfalls in image interpretation. This leads to both false positive and false negative diagnoses of clinically significant prostate cancer.<sup>1-4</sup> Knowledge of their clinical presentation and imaging appearances can help accurate image interpretation and guide clinical referrers to optimal management. In this review, we present common non-malignant pathologies of the prostate and SVs and discuss the clinical presentation and their imaging appearances in different imaging modalities.

## Benign Prostatic Hyperplasia

Benign prostatic hyperplasia (BPH) refers to an increase in the number of prostatic stromal and epithelial cells in the transition zone (TZ) and periurethral glands that cause the formation of discrete nodules and prostate enlargement.<sup>5</sup> It develops in response to testosterone after it is converted to dihydrotestosterone.<sup>6</sup> Its prevalence increases with age and affects approximately 75% of men older than 70 years.<sup>5</sup> BPH can cause bladder outlet obstruction leading to lower urinary tract symptoms like urgency, frequency, weak stream, and nocturia.

Imaging modalities in BPH include transabdominal ultrasound, transrectal ultrasound (TRUS), and MRI. Computed tomography (CT) scan has limited value as it does not accurately define prostatic zonal anatomy. Transabdominal ultrasound is the standard first-line investigation for BPH and shows an increase in a prostate volume exceeding 25cc. The central gland is enlarged with hypoechoic or mixed

DOI <https://doi.org/10.1055/s-0044-1779513>.  
ISSN 2581-9933.

© 2024. The Author(s).

This is an open access article published by Thieme under the terms of the Creative Commons Attribution License, permitting unrestricted use, distribution, and reproduction so long as the original work is properly cited. (<https://creativecommons.org/licenses/by/4.0/>)

Thieme Medical and Scientific Publishers Pvt. Ltd., A-12, 2nd Floor, Sector 2, Noida-201301 UP, India

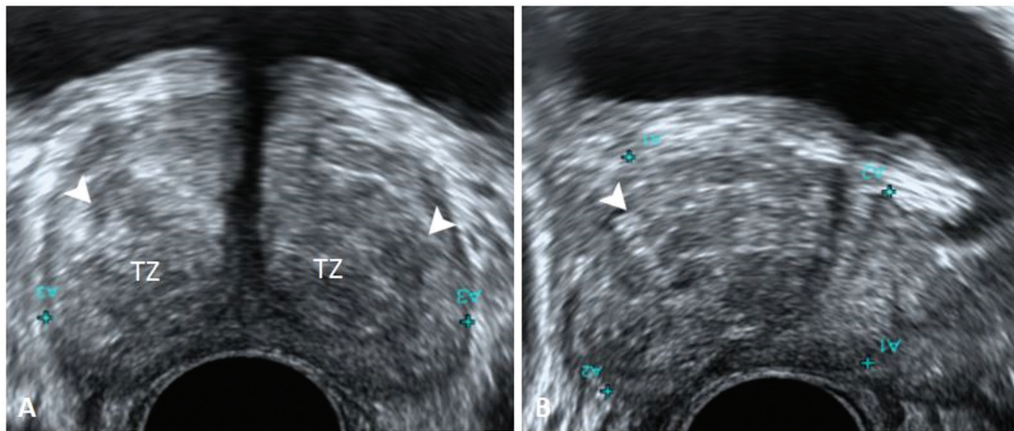


**Fig. 1** A 73-year-old man with lower urinary tract symptoms. Axial (A) and sagittal (B) transrectal ultrasound images showing enlargement of the bilateral transition zone with heteroechoic benign prostatic hyperplasia nodules (arrowheads).

echogenicity. There may be significant postvoid residual urine and associated bladder wall hypertrophy and trabeculations due to chronic bladder outflow obstruction.

On TRUS, BPH appears as a diffuse or nodular enlargement of the TZ, periurethral glandular tissue, or both.<sup>7</sup> Hyperplastic nodules are usually hypoechoic to peripheral zone (PZ) tissue but may be isoechoic or hyperechoic depending on the amount of fibrous, muscular, and glandular hyperplastic elements and are surrounded by fibrous envelopes that appear as hypoechoic rims (►Fig. 1).<sup>7</sup> On MRI, BPH

appears as band-like areas and/or encapsulated circumscribed round nodules in the TZ. While predominantly glandular nodules appear T2 hyperintense, stromal nodules may appear T2 hypointense and contribute to a substantial number of PIRADS 3 lesions in clinical practice.<sup>6</sup> The heterogeneous appearance of TZ on T2 due to both hyperintense and hypointense BPH nodules is likened to “organized chaos” (►Fig. 2). BPH nodules showing complete T2 hypointense rim are categorized as typical BPH nodules (PIRADS 1), while those showing partial encapsulation are atypical nodules

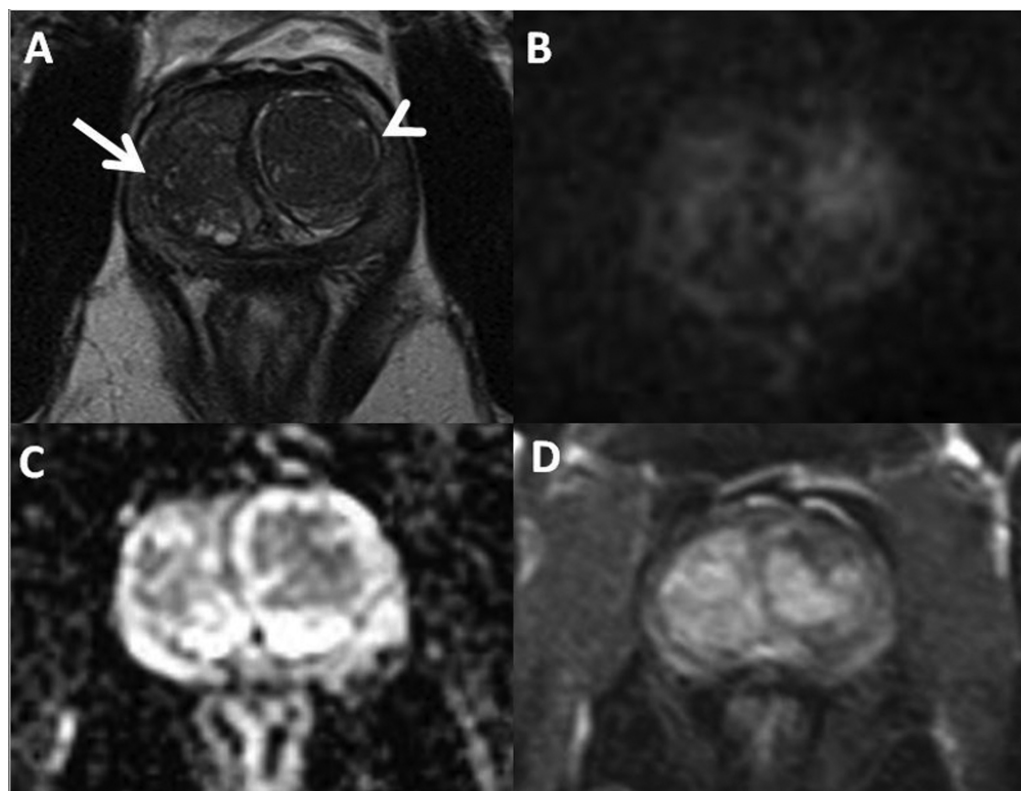


**Fig. 2** A 66-year-old male with lower urinary tract symptoms. T2 image in the axial plane (A) showing an enlarged transition zone with few well-encapsulated (arrowhead) and partly encapsulated (arrow) benign prostatic hyperplasia nodules. These nodules can be hyperintense if the glandular element predominates or hypointense if the stromal element predominates. The admixture of these nodules creates an “organized chaos” pattern. Diffusion-weighted imaging at b1500 (B) and apparent diffusion coefficient map (C) showing parts of this nodule showing restricted diffusion. Postcontrast image (D) showing early enhancement of these nodules.

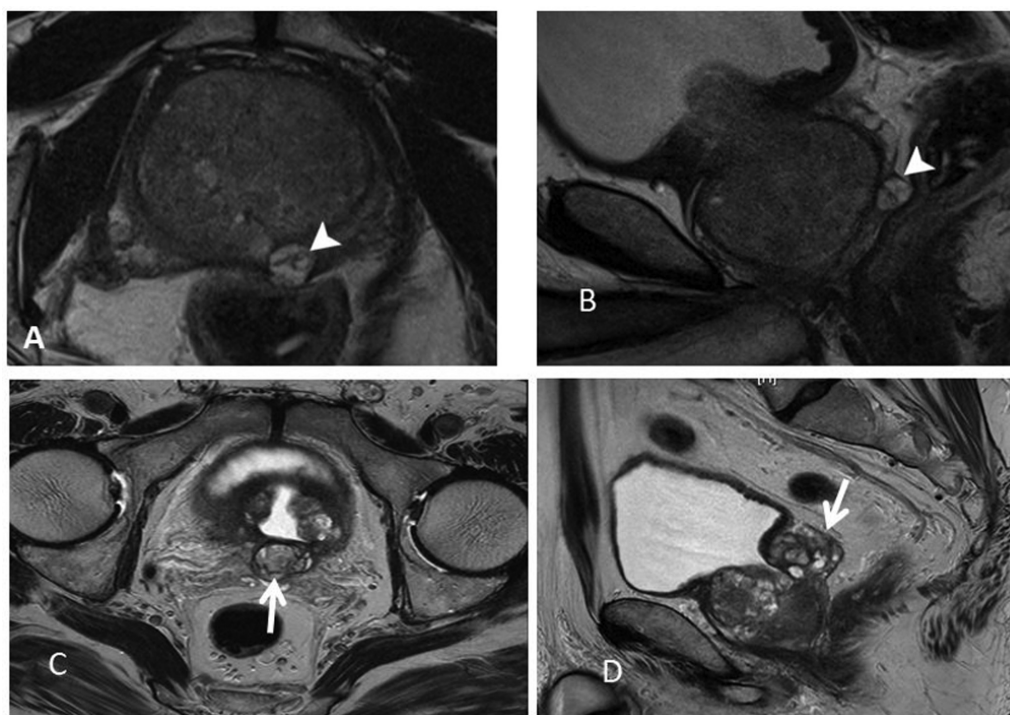


**Fig. 3** Extruded nodules in two different patients. Axial (A) and sagittal (B) T2-weighted magnetic resonance imaging (MRI) of the prostate in a 64-year-old man with an enlarged prostate and raised prostate-specific antigen (9.65ng/mL) showing benign prostatic hyperplasia (BPH) changes in the transition zone with retrourethral protrusion into the bladder. There is an extruded BPH nodule seen in the left posteromedial peripheral zone of the gland (arrowheads in A and B). Axial (C) and sagittal (D) T2-weighted MRIs of the prostate in another 75-year-old male who had transurethral resection of the prostate previously showing a well-encapsulated extruded heterogeneous nodule in the central zone of the gland (white arrows).

(PIRADS 2). Diffusion-weighted imaging (DWI) helps in differentiating BPH nodules from prostate cancer, as they do not show marked restricted diffusion on high b Value DWI ( $b \geq 1400$ ) or marked hypointensity on apparent diffusion coefficient (ADC) images. On dynamic contrast-enhanced MRI (DCE-MRI), BPH nodules may show early enhancement, hence it is unreliable. Although BPH nodules typically occur in TZ, exophytic or extruded BPH nodules can be seen in the peripheral zone (▶ Fig. 3) or central zone<sup>3</sup> and share a similar MRI appearance. ▶ Table 1 shows the types of BPH based on ultrasound and MRI findings.

Early disease is managed conservatively with alpha-blockers and 5-alpha reductase inhibitors. Surgical management for

symptomatic patients is achieved with transurethral resection of the prostate (TURP). Laser-based and thermal ablation procedures and prostatic artery embolization may also reduce periurethral prostatic volume and obstruction.<sup>8</sup> Any procedure that does not completely remove the TZ has the potential for recurrence and may result in the need for an additional procedure.

### Infections and Inflammatory Diseases

Prostatitis is inflammation or infection of the prostate and clinically presents with symptoms referable to the lower urogenital tract and perineum. Studies suggest the prevalence

**Table 1** Classification of BPH based on ultrasound and MRI findings<sup>8-10</sup>

Type 0	Normal prostate with volume <25cc
Type 1	Bilateral TZ enlargement
Type 2	Retro urethral enlargement also called median lobe hypertrophy
Type 3	Bilateral TZ and retro urethral enlargement
Type 4	Pedunculated intravesical prostatic protrusion, enlarged single or multiple nodules arising from intraluminal urethral submucosa
Type 5	Bilateral TZ and/or retro urethral enlargement with pedunculated intravesical protrusion of prostate
Type 6	Sub trigonal or ectopic enlargement
Type 7	Other combination of enlargements

Abbreviations: BPH, benign prostatic hyperplasia; MRI, magnetic resonance imaging; TZ, transition zone.

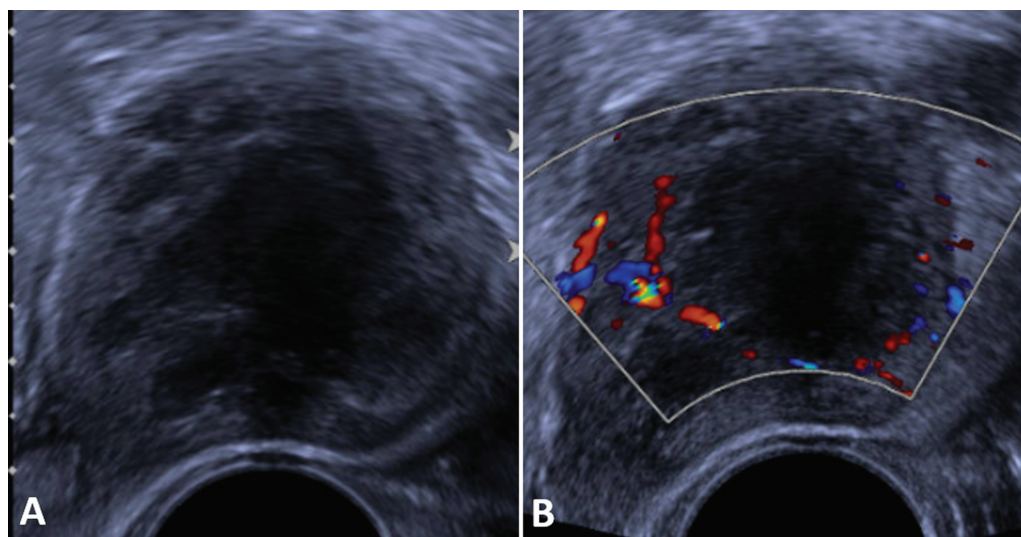


**Fig. 4** Transrectal ultrasound (TRUS) performed for a patient in sepsis shows enlarged prostate with irregular hypo echoic area (A) representing abscess. There is hyper-vascularity noted at the periphery of the gland (B) suggestive of prostatitis.

of prostatitis is 2 to 16%.<sup>11</sup> The National Institutes of Health classifies prostatitis into four categories—acute bacterial prostatitis, chronic bacterial prostatitis, chronic prostatitis or pelvic pain syndrome, and asymptomatic inflammatory prostatitis.<sup>12</sup>

#### Acute Prostatitis

Acute prostatitis has a bimodal age distribution affecting men of 20 to 40 years and over 60 years.<sup>13,14</sup> The most common pathogen is *Escherichia coli* (in ~60%), followed by *Pseudomonas aeruginosa* and Enterococcus species.<sup>15,16</sup> The infection spreads as ascending urethral infection, direct seeding from prostatic biopsy, intraprostatic reflux of infected urine, or by hematogenous spread as in sepsis and tuberculosis. About 6% of acute bacterial prostatitis can progress to prostatic abscesses in whom imaging is indicated.<sup>17</sup> Patients with acute prostatitis who do not respond to treatment after 48 hours should be evaluated for a possible prostatic abscess.<sup>18</sup>

Prostatic abscess appears as a hypoechoic area with internal septae and thick well-defined walls on TRUS (→Fig. 4); TRUS is also of value in ultrasound-guided drainage

of abscess (at least 18G needle is preferred). Unroofing/transurethral drainage of the prostatic abscess is preferred in lesions too large to drain percutaneously or lesions that do not respond to percutaneous drainage.<sup>19</sup> Contrast-enhanced CT shows an edematous appearance of prostate and periprostatic stranding. Prostatic abscess appears as hypodense focus with peripheral enhancement and internal septations (→Fig. 5).<sup>20</sup> Cross-sectional imaging also gives valuable information regarding extraprostatic spread. MRI offers better soft tissue resolution than CT and is more sensitive than TRUS in the early stages of abscess formation. Abscess shows a low signal on T1, high signal on T2-weighted MRI, central diffusion restriction and displays peripheral rim enhancement with gadolinium.<sup>20</sup>

Prostate must be carefully reviewed in patients with cystitis with persistent fever in the absence of upper urinary tract infection (UTI), recurrent UTI in the absence of renal involvement/structural abnormalities of the urinary tract, secondary peritonitis, immunocompromised, diabetic patients, and those with sepsis (→Figs. 1 and 2). Prostatic abscess carries high morbidity and mortality and needs a

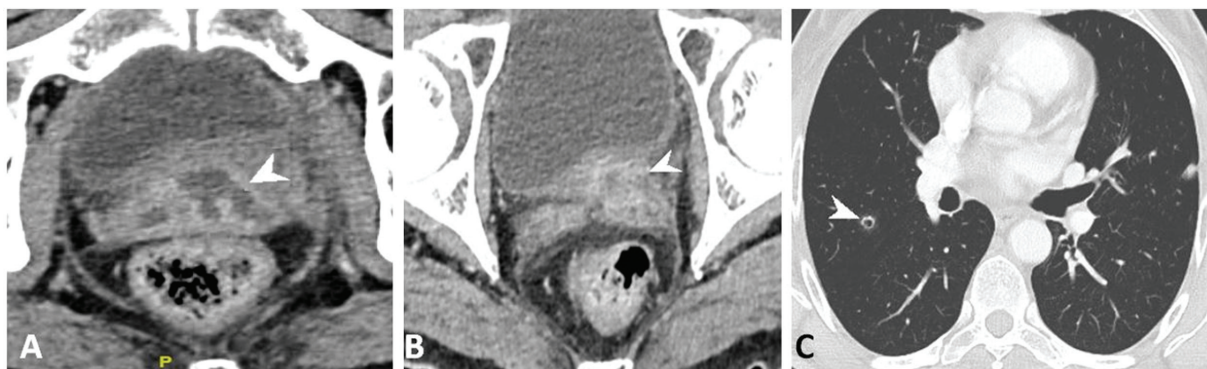


**Fig. 5** A 61-year-old male with sepsis. (A, B) Axial computed tomography (CT) image showing irregular branching hypodense collections in the prostate and seminal vesicles (arrowheads) with periprostatic fat stranding. There is a contiguous thickening of the bladder base. (C) Selected high-resolution CT images of the same patient showed multiple septic emboli in the lungs seen as cavitating nodules (arrowhead).

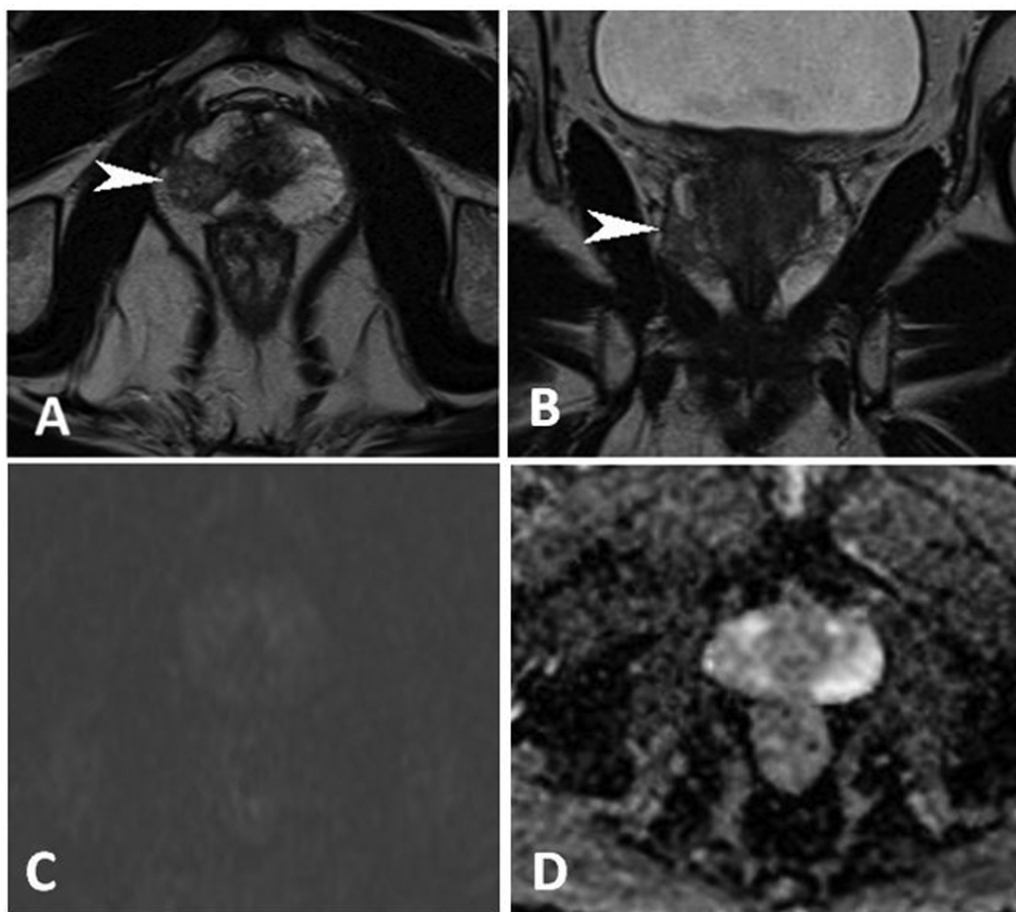


**Fig. 6** A 65-year-old male with lower urinary tract symptoms, an enlarged prostate gland, and a hard right-sided nodule palpable on clinical examination. Prostate-specific antigen was 0.88 IU/mL. (A, B) High-resolution T2 axial and coronal images showed a wedge-shaped T2 hypointense lesion with a striated appearance in the antero-lateral and postero-lateral peripheral zone in the right mid-gland. (C, D) Diffusion-weighted imaging (b1500) and apparent diffusion coefficient map showed no diffusion restriction. Based on these imaging features, magnetic resonance imaging was reported as PIRADS 2, likely changes of chronic prostatitis.

high index of suspicion, and imaging is critical for timely diagnosis and treatment.

### Chronic Prostatitis

It encompasses a spectrum of etiologies from a sequel to acute prostatitis, and recurrent UTIs to IgG4-related disease and tuberculous prostatitis. Chronic prostatitis appears as wedge-shaped T2 hypointense lesions with a linear pattern in the peripheral zone with or without capsular retraction and does not show diffusion restriction (►Fig. 6). Granulomatous prostatitis (GP) is a nodular form of chronic prostatitis. It can be idiopathic, tuberculous, iatrogenic due to Bacille Calmette-Guerin (BCG) vaccine, intravesical BCG for bladder cancer, postradiotherapy or due to autoimmune aetiologies and systemic conditions like sarcoidosis.<sup>21</sup> GP demonstrates a tumor-like morphology, with nodular or diffuse hypoechoic lesions on ultrasound, and has PIRADS 5 appearance on mpMRI.<sup>22</sup> On T2-weighted MRI, GP lesions appear hypointense like prostate cancer. GP and cancer lesions share high signal intensity on high b-value DWI and low signal intensity on the ADC map. On DCE-MRI, GP shows moderate persistent enhancement and prostate cancer shows early enhancement and rapid washout due to

increased vascularity.<sup>23</sup> GP is more commonly diffuse when compared to prostate cancer. Unlike the diffuse forms of prostate cancer, in GP the prostatic capsule is usually intact (►Fig. 7). Clinical profile combined with declining serial prostate-specific antigen (PSA) value in some cases may hint the radiologist to a diagnosis of GP over malignancy.

### Prostatic and Periprostatic Cysts and Their Mimics

Prostatic and periprostatic cysts are uncommon pathologies often encountered as incidental findings on imaging.<sup>24</sup> These are mostly asymptomatic but sometimes may present with lower urinary tract symptoms and infertility.<sup>24</sup> Knowledge of embryology and anatomical localization by high-resolution MRI helps in characterizing these lesions.

#### i) Prostatic cysts

##### *Prostatic Utricle and Müllerian Duct Cysts*

The Müllerian duct is an embryonic structure that normally regresses in males, except for a part at its cephalic end that contributes to remnant structures such as the prostatic utricle and testicular appendix.<sup>25</sup> A prostatic utricle cyst is

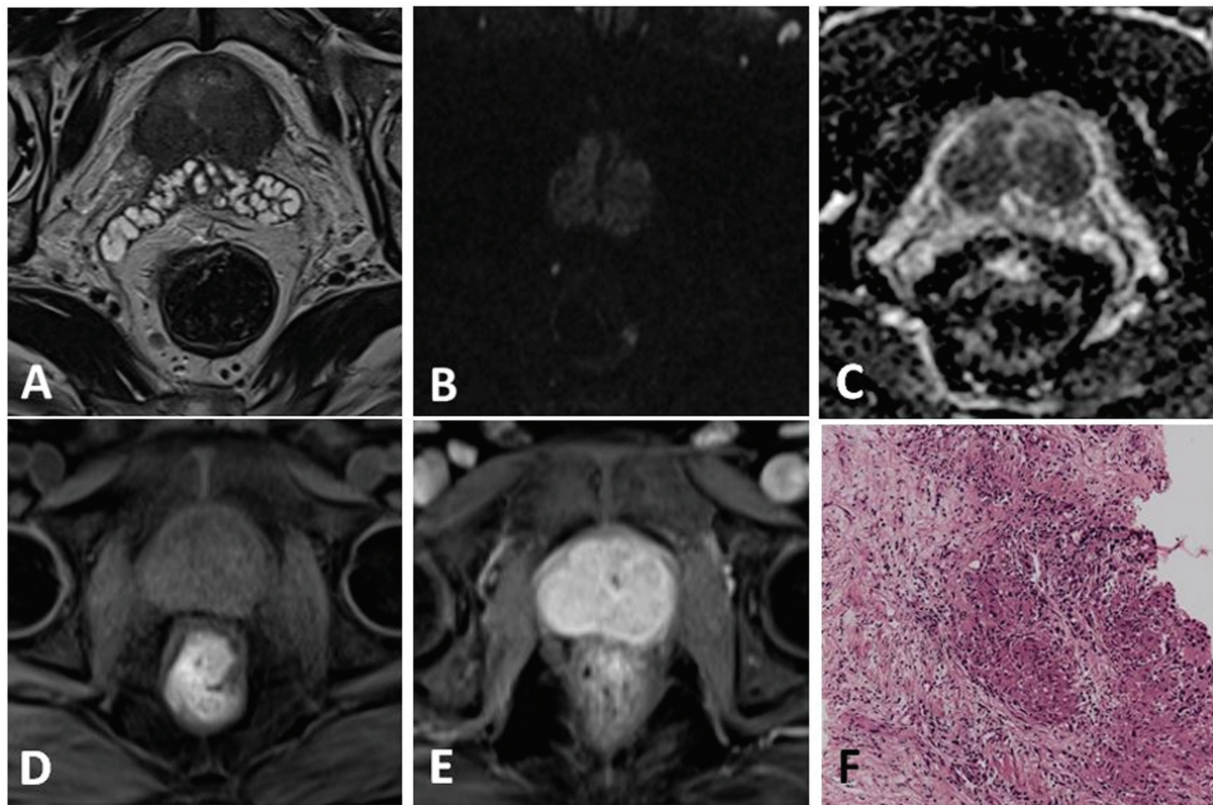


**Fig. 7** A 58-year-old male with prostate-specific antigen (PSA) of 5 IU/mL from elsewhere and a repeat PSA at our center 8 weeks after the previous PSA of 1.64 IU/mL. Multi-parametric magnetic resonance imaging (MRI) of the prostate was done. (A) T2-weighted axial image showed diffuse T2 hypointense signal of the prostate gland. The capsule was smooth and there was no seminal vesicle involvement. (B, C) Diffusion-weighted imaging showed diffusely hyperintense prostate gland on b-1500 image and low signal on apparent diffusion coefficient map suggestive of diffusion restriction. (D, E) Select images of dynamic contrast-enhanced MRI have shown diffuse intense enhancement of the prostate gland. (F) Transrectal ultrasound -guided biopsy showed prostatic parenchyma with aggregates of epithelioid histiocytes forming discrete granulomas (hematoxylin and eosin x 100).

a cystic dilatation of the prostatic utricle. Müllerian duct cysts are cystic dilatations of segments of the Müllerian duct that failed to regress.

Ultrasonography, CT, and MRI can detect these cysts. The anatomic location, shape of the cyst, and relationship with the urethra can aid in distinguishing between prostatic utricle cyst and Müllerian duct cyst as summarized in **Table 2**. MRI has the advantage of superior soft tissue resolution and high-resolution images can assess relationships with adjacent structures better (**Fig. 8**).<sup>26,27</sup>

Management decisions are based on the size of the cyst, its location, and the symptoms of the patient. Cysts larger than

2.5 cm are usually symptomatic and may need urology referral and further management. These cysts can bleed or get secondary infection and very rarely can transform into malignancy.<sup>26</sup> Management options for Müllerian duct cysts include surveillance, TRUS-guided aspiration and injection of sclerosing agents, surgical excision, transurethral resection, and percutaneous aspiration. Laparoscopic excision has also been tried.<sup>24,27</sup>

*Ejaculatory duct cysts*

Ejaculatory duct cysts usually develop secondary to ejaculatory duct obstruction<sup>25</sup> and can be congenital or acquired.<sup>24</sup> The ejaculatory duct is a short, approximately

**Table 2** Imaging differences between prostatic utricle cysts and Müllerian duct cysts

	Prostatic utricle cyst	Müllerian duct cyst
Location	Always in midline location	Can extend to a slightly para-midline location
Extension above prostate	No	Yes
Communication with the urethra	shows communication with the urethra	no communication with the urethra
Configuration	Pear shape	Tear drop shape
Contents on aspiration	May contain sperms within	Sperms are not seen. However, occasionally contain calculi

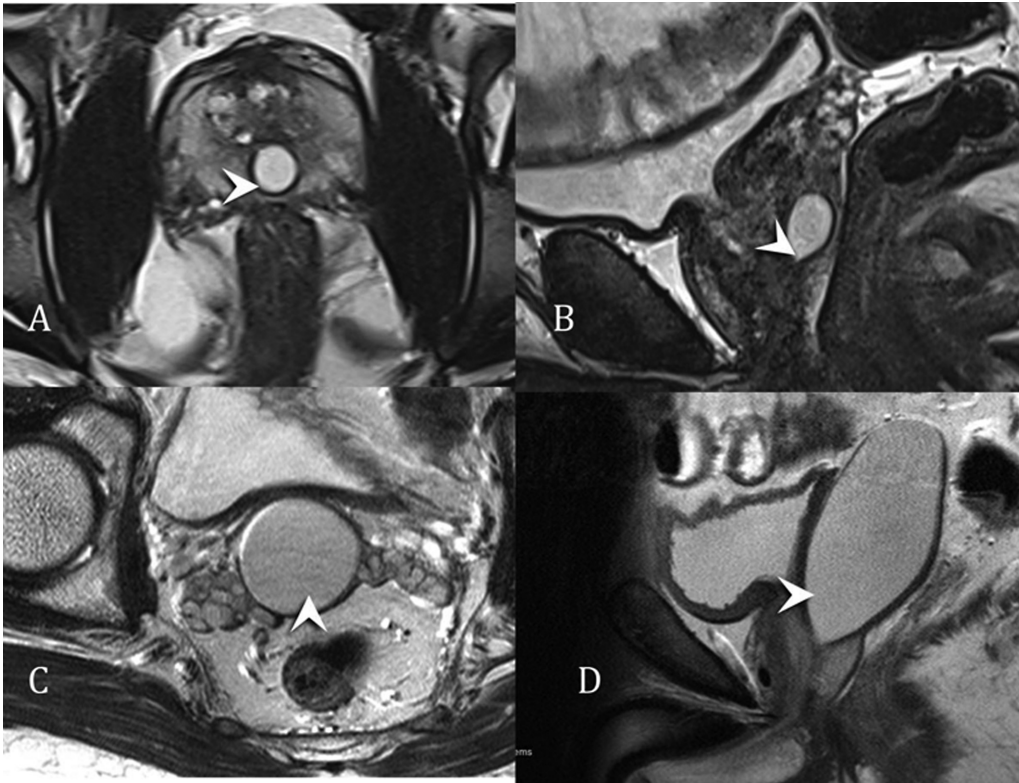


**Fig. 8** Prostatic utricle cyst in a 56-year-old man. Axial (A) and sagittal (B) high-resolution T2-weighted (T2W) magnetic resonance imaging (MRI) showing a midline cystic lesion (arrowhead) at the level of verumontanum (arrowhead). (C, D) Müllerian duct cyst in a 37-year-old patient with recurrent urinary tract infections. Axial (C) and sagittal (D) high-resolution T2W MRI showing a large, elongated midline hyperintense lesion (arrowhead) extending above the prostate.

2 cm long structure coursing through the central zone of the prostate gland and formed by the joining of duct from the SV and ductus deferens. On imaging, these are seen as paramedian cysts (–Fig. 9A, B) in the central zone along the ejaculatory duct.<sup>25</sup> Larger lesions may extend above the prostate gland and appear as midline lesion.<sup>25,26</sup> The obstructed ejaculatory duct causes proximal dilatation of the duct depending on the level of obstruction and extent of fibrosis. There can also be ipsilateral prominence of vas deferens, dilatation of SV ducts, and enlargement of SV. High-resolution MRI is helpful in localizing the level of obstruction.<sup>25</sup> Due to limited availability and cost factors,

MRI is reserved for cases with inconclusive ultrasonography.<sup>25</sup> Aspirate shows spermatozoa, and fructose and may rarely contain calculi.<sup>26</sup> The treatment is usually surveillance and surgery is considered in symptomatic patients or those with infertility.

*Prostatic retention cysts (PRC) and cystic degeneration of BPH* These are usually seen in the region of glandular tissues of the prostate gland, mostly asymptomatic, and encountered during the 5th to 6th decades of life.<sup>25</sup> The exact etiology of PRC is unknown, but is seen frequently in patients with BPH<sup>25</sup> and could be the result of obstruction of the prostatic parenchymal ductules.<sup>26</sup> On imaging, these are round,

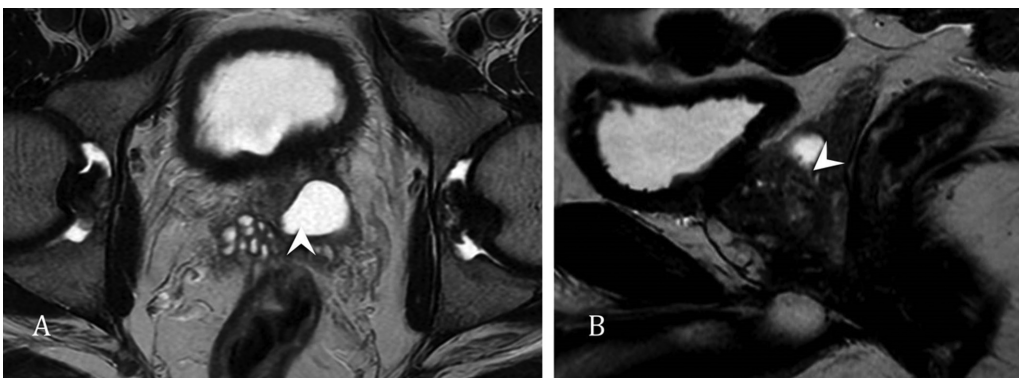


**Fig. 9** Incidentally detected ejaculatory duct cyst in 48-year-old gentleman for the evaluation of rectal polyp. Axial (A) and sagittal (B) high-resolution T2-weighted magnetic resonance imaging showing a left paramedian cyst (arrowhead) in the central zone along the ejaculatory duct above the level of verumontanum.

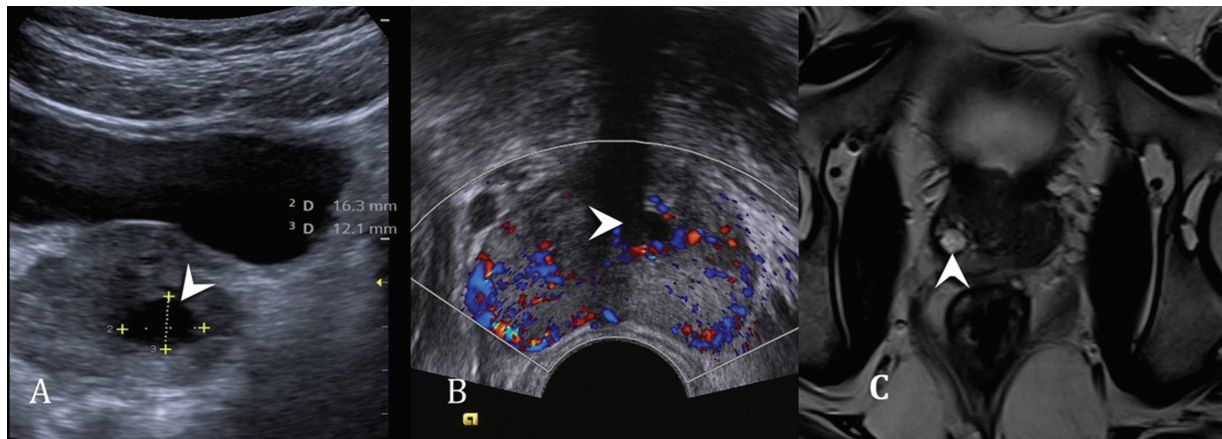


**Fig. 10** (A, B): A 62-year-old gentleman with bladder outlet obstruction symptoms. Trans-abdominal ultrasound (A) and transrectal ultrasound (B) showing an enlarged prostate with an anechoic lesion in the left transition zone in the mid-gland level (arrowhead) likely cystic degeneration of benign prostatic hyperplasia. (C) Axial high-resolution T2 magnetic resonance imaging showing a well-defined unilocular cyst in the right posterolateral peripheral zone (arrowhead) at mid-gland level that was incidentally detected in a patient with left renal agenesis suggestive of a prostate retention cyst.

smooth unilocular cysts and can occur in any prostatic zone, usually the peripheral zone with or without background changes of BPH (► Fig. 10A, B). Cystic degeneration of BPH nodules results in irregularly shaped cysts commonly seen in the TZ of the prostate gland (► Fig. 10C).

**Tumoral cysts**

Some tumors like multilocular prostatic cystadenoma and adenocarcinoma also show cystic changes along with soft tissue components.<sup>24,28</sup>

**ii) Periprostatic cysts**

Periprostatic cysts include SV cysts, cyst of vas deferens, and Cowper’s duct cysts.<sup>24</sup>

**Seminal vesicle cysts**

These can be congenital or acquired and may be associated with adult polycystic kidney disease.<sup>26,27</sup> These are mostly detected incidentally unless they are large enough to cause obstructive urinary symptoms.<sup>29</sup> They occur commonly in

sexually active males secondary to a malformed or stenosed duct system.<sup>27</sup> When congenital, they develop due to atresia of ejaculatory ducts and thereby, are associated with bulky distended SV. Congenital cysts are mostly unilateral and associated with anomalies like renal agenesis, ectopic ureteric insertion, and vas deferens agenesis. Zinner syndrome is a triad of unilateral renal agenesis, ipsilateral SV cyst, and ejaculatory duct obstruction<sup>27</sup> (► Fig. 11). On imaging, they appear as well-defined round/oval/tubular cysts within the SV, posterior to the urinary bladder.<sup>26,29</sup> In cases of hemorrhage and proteinaceous content, they appear hyperintense on T1-weighted imaging and hypointense to bladder contents on T2 weighted imaging (► Fig. 11).<sup>27</sup> On TRUS, they are seen as anechoic cystic lesions within the SV with variable echogenicity in the presence of hemorrhage or proteinaceous content.<sup>27,29</sup> These cysts are usually treated with conservative management. However, TRUS-guided cyst drainage can be done if symptomatic.<sup>27</sup>

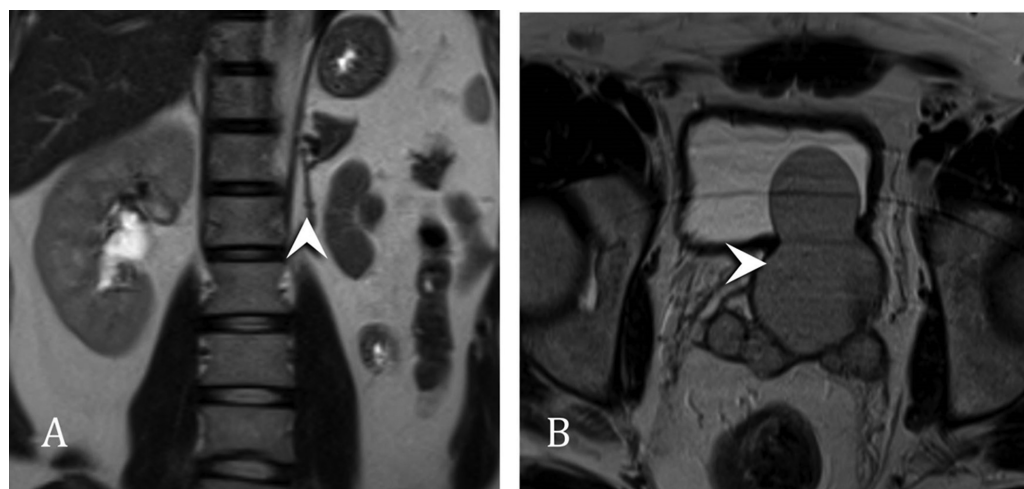


**Fig. 11** A 33-year-old gentleman with infertility. Coronal (A) high-resolution T2-weighted (T2W) image of the abdomen showing left renal agenesis (arrowhead), and axial (B) high-resolution T2W magnetic resonance image of the pelvis showing ipsilateral seminal vesicle cyst (arrowhead) indenting the left posterior wall of the urinary bladder, suggestive of Zinner syndrome.



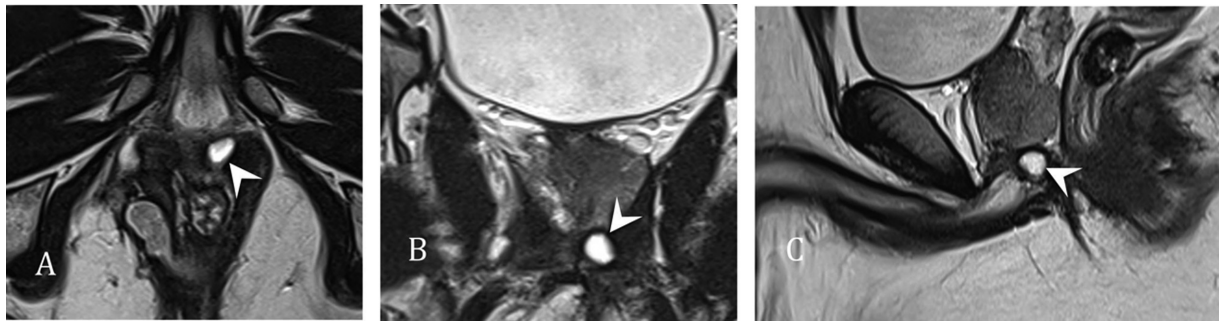


**Fig. 12** Incidentally detected Cowper's duct cyst in a 38-year-old gentleman with rectal bleeding. Axial (A), coronal (B), and sagittal (C) high-resolution T2-weighted images of the prostate showing a small ovoid hyperintense lesion at the base of the penile urethra, posterior to the posterior urethra and inferior to the prostate apex.

#### *Cysts of the vas deferens*

Ductus deferens, formerly called vas deferens, is a muscular tube that transports sperm from epididymis to ejaculatory ducts. These cysts are seen along the ductus deferens and cranial to the prostate gland and posterior to the urinary bladder.<sup>27,28</sup> On MRI, these are seen as well-defined T1 hypointense, T2 hyperintense fluid signal thin-walled cysts and are not easily confused with other differentials<sup>26,27</sup> due to their location along the course of the ductus deferens.

#### *Cowper's (bulbourethral) duct cysts*

Cowper's glands are paired structures located on either side of the urogenital diaphragm at the level of the membranous urethra.<sup>30</sup> Secretions from each gland drain into individual ducts that join to form a single duct that empties into the

proximal bulbar urethra.<sup>31</sup> The dilatation of the duct called syringocele is very rare and develops due to duct obstruction. Based on its communication with the urethra, it is divided into open type and closed type.<sup>30</sup> These can be congenital or acquired, and encountered more often in pediatric population. The majority of them are asymptomatic. Symptoms if present include recurrent UTIs, voiding problems, dysuria, and palpable perineal mass.<sup>32</sup> On imaging, these are seen as well-defined midline or paramedian cysts that appear anechoic on ultrasound and hyperintense on T2-weighted MRI, located posterior to the posterior urethra and inferior to the prostatic apex<sup>27</sup> (→**Fig. 12**). Asymptomatic or mildly symptomatic cases are kept under surveillance and patients with severe symptoms are managed by endoscopic derroofing of



**Fig. 13** Mimics of prostatic and periprostatic cysts. (A, B) A 72-year-old with post-transurethral resection of the prostate (TURP) status. Axial (A) and coronal (B) high-resolution T2-weighted images showing post-TURP defect (arrowhead). Axial computed tomography (C) images of a 62-year-old gentleman showing a large urinary bladder diverticulum along left lateral aspect of the bladder (arrowhead), which shows communication (D) with the urinary bladder (arrowhead).

**Table 3** Differentiating features of various mimickers of prostatic and periprostatic cysts

Mimics	Imaging	Is it difficult to differentiate?
Defect from transurethral resection of prostate:	Funnel-shaped irregular defect in the mid part of upper end of prostate. It is seen communicating with the urinary bladder	Easily identified as a defect rather than a cystic lesion in the appropriate clinical setting
Hydroureter and ectopic insertion of ureter:	Hydroureter with tortuous course can look like a periprostatic lesion. Ectopic insertion of the ureter into the prostatic part of the urethra can also mimic a periprostatic cyst	Evaluation in multiple planes is helpful in the diagnosis
Urinary bladder diverticulum:	These mimic periprostatic cysts when located along the prostate or seminal vesicle	Communication of these cysts with the urinary bladder confirms the diagnosis

the cyst. Other options include endoscopic/ open trans-perineal excision or ligation of the cyst<sup>33</sup>

### iii) Mimics of prostatic and periprostatic cysts

Ureterocele, dilatation of the prostatic urethra after TURP, bladder diverticula, hydroureter and ectopic insertion of the ureter (► Fig. 13) are mimickers of prostatic and periprostatic cysts and the differentiating features<sup>2,4</sup> have been tabulated in ►Table 3.

## Benign Neoplasms of Prostate and Seminal Vesicles

A wide variety of neoplasms, both benign and malignant can occur in the prostate and SV.<sup>34</sup> Malignant neoplasms are

much more common than benign neoplasms, with acinar adenocarcinoma being the most common neoplasm. Benign neoplasms are of mesenchymal origin and constitute less than 1% of all tumors.<sup>35</sup> They generally are large lesions that cause nonspecific and chronic lower urinary tract symptoms. PSA levels will usually be normal in these neoplasms because PSA is produced by epithelial cells of the prostate, which enter the bloodstream when the blood epithelial barrier is destroyed.

### Stromal Tumors of Uncertain Malignant Potential

Prostatic stromal tumors of uncertain malignant potential (STUMPs) are rare stromal tumors with unpredictable biological behavior. They are reported to occur in adults of any age, with the highest prevalence in the 6<sup>th</sup> to 7<sup>th</sup> decades.<sup>34</sup>

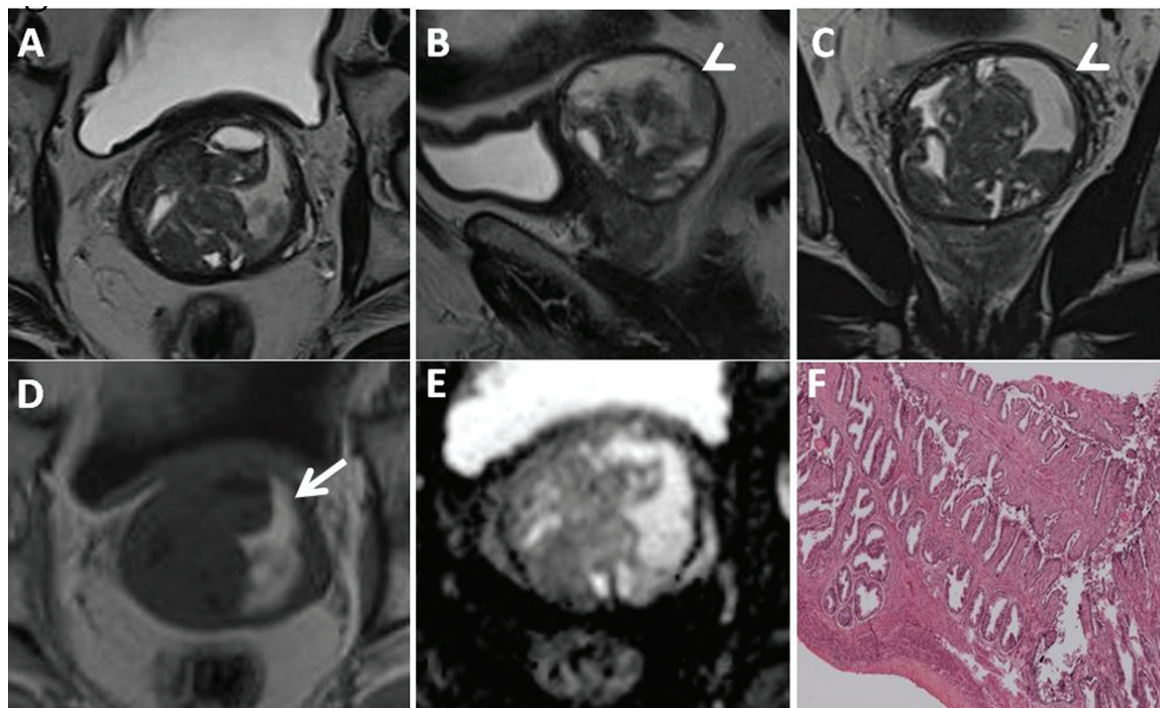


**Fig. 14** Stromal tumor of uncertain malignant potential (STUMP) in a 66-year-old male. T2 image in axial (A), sagittal (B), and coronal (C) planes showing a well-circumscribed solid-cystic lesion arising from the posterior peripheral zone of the prostate gland with a rim-like T2 hypo-intense “capsule” (arrowhead in B and C). The T1 image in the axial plane (D) showing that the cystic areas are T1 hyperintense suggesting blood products (arrow in D). Apparent diffusion coefficient map (E) showing no diffusion restriction. Histopathology microphotograph (F) confirms the diagnosis of STUMP showing complex branching glands and increased stromal cellularity (hematoxylin and eosin x 40).

Based on the histologic appearance, there are five patterns of STUMPs.<sup>34</sup> The most common pattern is a lesion with hypercellular stroma with scattered atypical but degenerative-looking cells admixed with benign prostatic glands. A distinctive pattern of STUMP is the phyllodes subtype, with a leaf-like growth pattern. Stromal tumors are positive for CD34 and progesterone receptors and uncommonly express estrogen receptors.

STUMPs commonly arise from the peripheral zone rather than the TZ of the gland and appear as a solitary, sharply circumscribed, solid or solid-cystic mass with solid areas showing T1 hypointense and T2 hyperintense signal (►Fig. 14) on MRI.<sup>36</sup> The cystic component can be clear fluid, mucinous, or blood. A rim-like hypointense “capsule” is characteristically seen on T2-weighted images (►Fig. 14). The solid components of the lesion show gradual enhancement on DCE-MRI. Large tumors may invade adjacent organs such as the rectum and there are case reports of metastases to the lungs and bones.<sup>37</sup> The differential diagnosis includes BPH nodules, cystadenoma (►Fig. 18), sarcomas, and other mesenchymal lesions. Treatment of STUMP is complete surgical resection; however, they frequently recur (up to 65%).<sup>37</sup>

### Benign Nonstromal Mesenchymal Tumors

Benign non-stromal mesenchymal tumors arise from smooth muscle elements in prostatic stroma or periglandular tissue. Leiomyoma, schwannoma, solitary fibrous tumor (SFT), inflammatory myofibroblastic tumor (IMT), and paragangliomas are benign mesenchymal tumors reported to arise from prostate and are very rare.<sup>36</sup> Generally, they have non-specific imaging features and need a biopsy for a definitive diagnosis. The differentiation between benign and malignant mesenchymal tumors also may be difficult unless there is definite evidence of local invasion or metastasis.

Leiomyoma arising within the gland can resemble the stromal nodule of BPH if it is small, though most of them are very large at presentation.<sup>38</sup> Imaging shows a well-defined, solitary, solid mass with predominantly homogeneous enhancement. At MRI, T1 and T2-weighted images have low signal intensity and homogeneous enhancement when small, but large lesion can be heterogeneous on T2 and postcontrast images due to necrosis (►Fig. 15). Expression of smooth muscle actin and desmin confirms the diagnosis, while CD34 is negative, distinguishing it from STUMP.<sup>39</sup>

Schwannomas typically arising in the 4<sup>th</sup> to 6<sup>th</sup> decades are commonly sporadic. A smaller proportion can be associ-

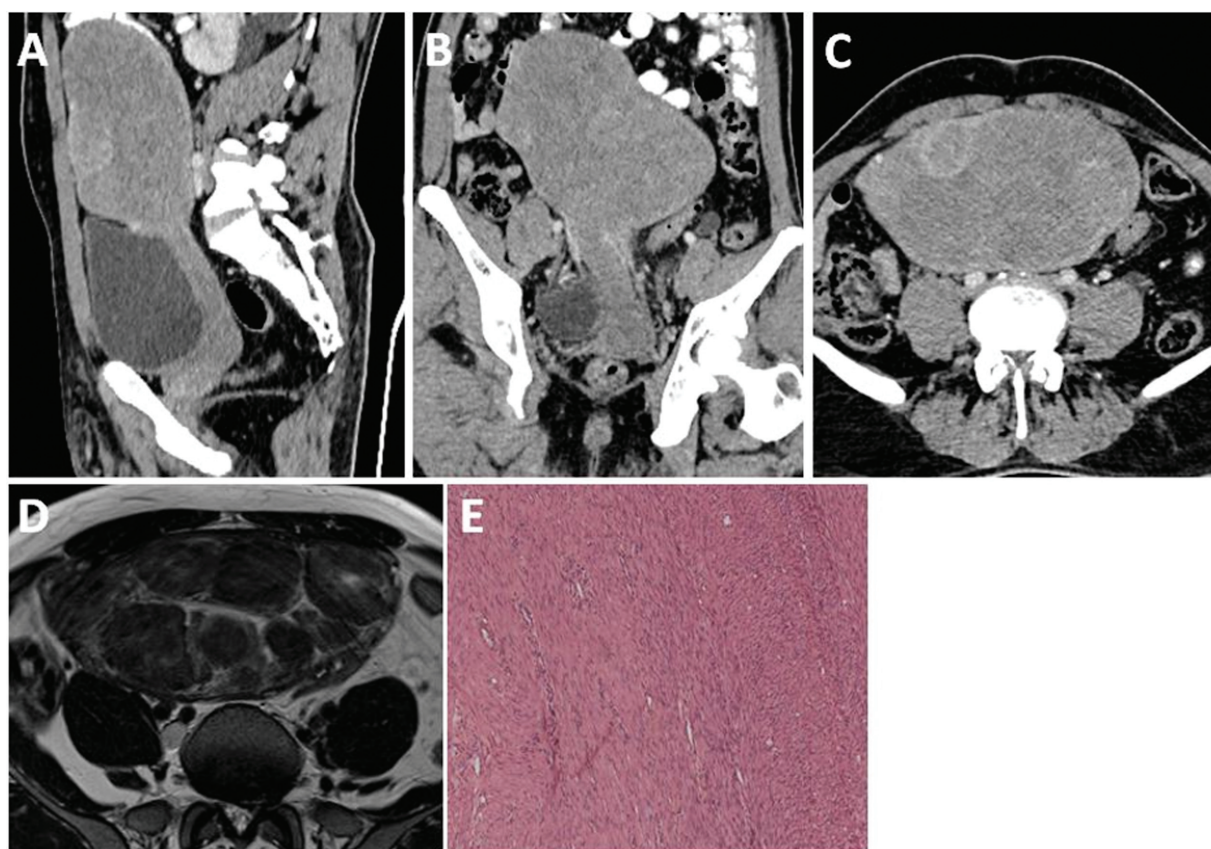


**Fig. 15** A 44-year-old male with a palpable paraumbilical mass on clinical examination. (A–C) Oblique sagittal, oblique coronal, and axial computed tomographic images of a well-margined, and pedunculated solid lesion arising from the left seminal vesicle showing heterogeneous enhancement with no invasion to adjacent structures. (D) High-resolution T2 axial images showed that the lesion is predominantly T2 hypointense. (E) Histopathology confirmed the diagnosis of leiomyoma of the seminal vesicle with fascicles of spindle cells with eosinophilic cytoplasm, blunt-ended oval nuclei, and minimal to no cytological atypia (hematoxylin and eosin x 100).

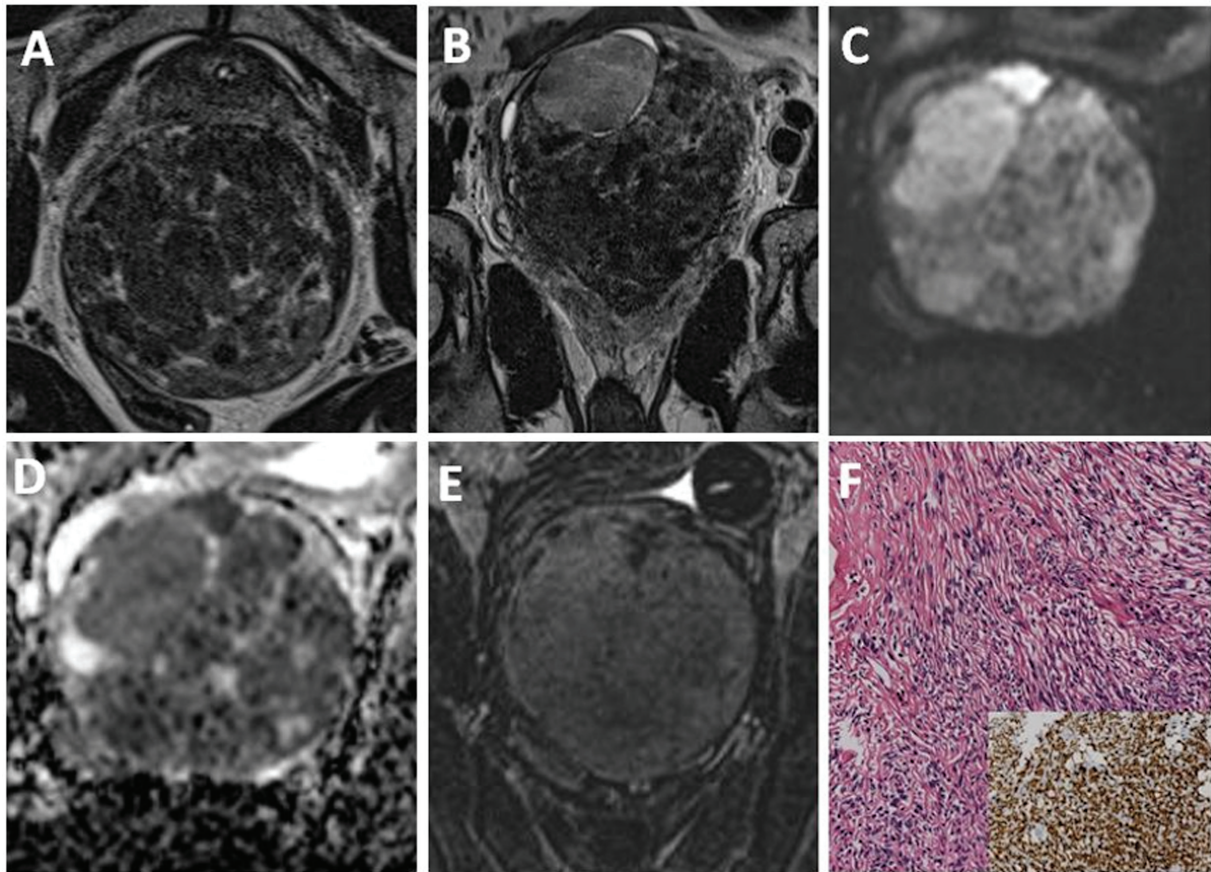


**Fig. 16** A 53-year-old male with acute painless urinary retention and an enlarged firm nontender prostate gland, on clinical examination. Prostate-specific antigen was 0.88 IU/mL. Multiparametric magnetic resonance imaging of the prostate. T2-weighted images in axial (A) and coronal (B) planes showed a well-defined lesion from the prostate with heterogeneously hypointense signal intensity. Diffusion-weighted imaging with b 1500 (C) and apparent diffusion coefficient (D) images showed areas of restricted diffusion. Delayed postcontrast subtraction image (E) reveals gradual enhancement. Histopathology microphotograph (F) diagnosed it to be a solitary fibrous tumor with variable cellularity, and dense hyalinized collagenous stroma (hematoxylin and eosin x 200). The tumor cells stained positive for STAT6 (Inset image in F).

ated with hereditary syndromes like neurofibromatosis type 2 and schwannomatosis.<sup>40</sup> On CT, sporadic schwannomas are typically well-circumscribed solitary oval masses with cystic changes, calcifications, and variable enhancement. MRI usually shows low T1 signal intensity, heterogeneous high T2 signal, and variable post contrast enhancement.<sup>41,42</sup>

SFT originating from prostate is rare and have been reported previously among different age group ranging from 21 to 75 years. They are generally large lesions over 5 cm and may induce paraneoplastic syndromes like hypoglycemia (Doege-Potter syndrome) due to tumor-secreted insulin-like growth factor-2.<sup>43,44</sup> On MRI, SFT appears hypointense on T1-weighted images and displays mixed heterogeneous signal intensity on T2-weighted images, dependent on collagen or other components. Gradual post enhancement is seen owing to fibrous content. Diffusion restriction may indicate areas of high cellularity (► Fig. 16).<sup>45</sup> Surgical removal remains the primary treatment; however, recurrence is reported in 10 to 30% of cases.<sup>46</sup>

Prostate IMT has been reported between ages 21 to 83 years.<sup>38,47</sup> They appear hypointense on T1-weighted images and mixed heterogeneous on T2-weighted images depending on fibrosis and inflammation. Contrast-enhanced CT and MRI can display avid, homogeneous, or heterogeneous enhancement.<sup>36</sup>

Prostate paragangliomas are rare tumors derived from extra-adrenal chromaffin cells in sympathetic or parasympathetic paraganglia. They can have sporadic or familial occurrences (linked to syndromes like MEN 2A/B, von

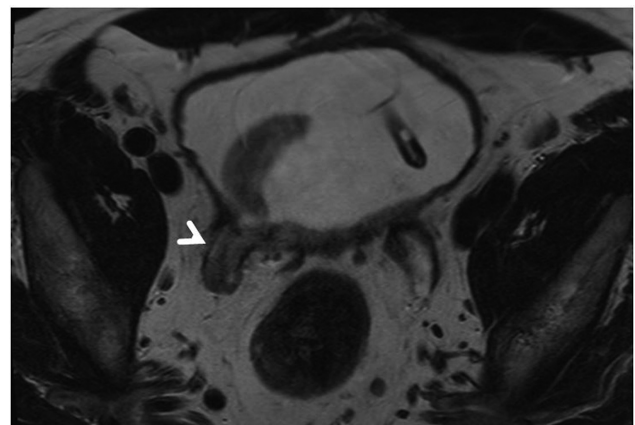


**Fig. 17** Ectopic prostate tissue in a patient who presented with right flank pain. T2 axial image showing concentric thickening (arrowhead) of the right terminal ureter. This was diagnosed to be prostate parenchyma on cystoscopy and biopsy. (This case was contributed by Prof. Mukesh Harisinghani, MGH, USA).

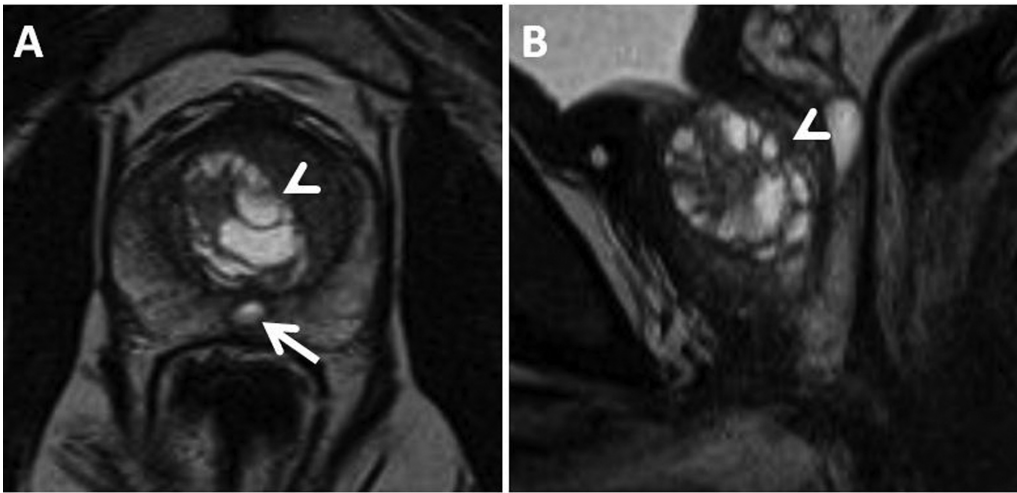


**Fig. 18** Prostate cystadenoma in a 40-year-old male. T2 image in axial (A) and sagittal (B) planes showing a well-encapsulated multiloculated cystic lesion (arrowheads in A and B) in the transition zone of the prostate with no solid areas. A small prostatic utricle cyst is seen in the posterior peripheral zone in the midline (arrow in A).

Hippel-Lindau, neurofibromatosis type 1, Carney complex, and familial paraganglioma syndromes). Functioning types may exhibit catecholamine-related symptoms.<sup>48,49</sup> In contrast to CT and MRI, paraganglioma appears as hyper enhancing lesion reflecting the richly vascularized nature of these tumors. At MRI, paragangliomas typically show

marked T2 hyperintensity with classic salt-and-pepper appearance due to multifocal signal voids. They tend to have high signal intensity at high b-value DWI, but the signal on the ADC map is not reduced or only mildly reduced. PET imaging with 68Ga DOTATATE will show marked avidity.<sup>49</sup>

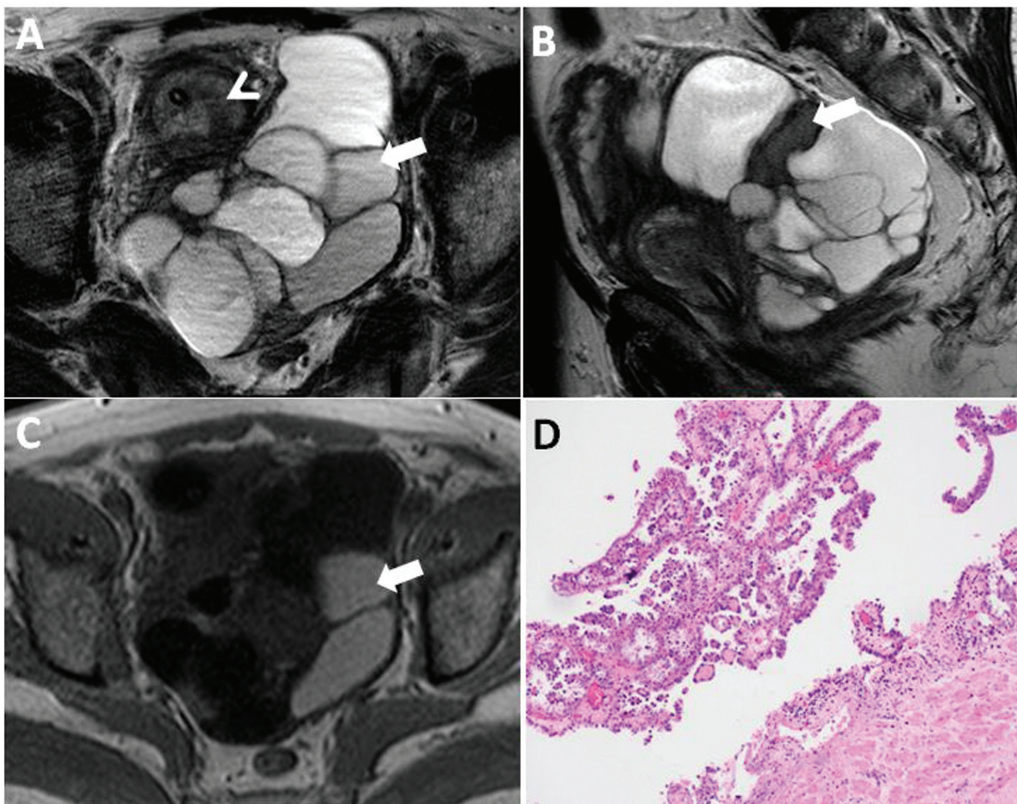


**Fig. 19** Seminal vesicle cystadenoma in a 57-year-old male. T2 images in the axial (A) and sagittal (B) planes and T1 images in the axial (C) plane showing a large encapsulated multiloculated cystic mass with no solid areas from the left seminal vesicle. The prostate is seen separately (arrowhead). The loculi of the tumor showing varying T1 and T2 signal intensities (arrows). Histopathology microphotograph (D) confirms the diagnosis and shows cyst wall and papillary structures lined by a single layer of cells (hematoxylin and eosin x 40).

### Ectopic Prostate Tissue

Ectopic prostatic tissue (EPT) is defined as the presence of prostatic tissue at sites other than the prostate. It is mostly reported in the urethra and bladder and less commonly reported in the genital tract involving SV, epididymis, and testis.<sup>50,51</sup> There are case reports of EPT described in other locations, including the bowel,<sup>52</sup> pelvis,<sup>53,54</sup> and spleen.<sup>55</sup> The origin of this around the lower urinary tract is believed to be vestigial remnants of developmental migration, while other sites may involve metaplasia or misplacement of prostate glands during development.<sup>51</sup> Clinical manifestations of EPT in the lower urinary tract include hematuria or urinary obstruction. EPT in the rest of the sites is either asymptomatic or has non-specific symptoms.<sup>51</sup> Prostate hyperplasia and neoplasms developing in EPT have been reported.<sup>51,52</sup> MRI shows the typical signal intensity of the prostate gland with or without hyperplasia and **Fig. 17** is an example of EPT in the right distal ureter. The symptomatic patients are managed surgically.

### Cystadenoma of the Prostate and Seminal Vesicle

Cystadenoma of the prostate and SV are rare benign multi-locular cystic tumors. Though the same nomenclature is used for both prostate and SV lesions, they are classified separately in the World Health Organization classification with some differences in pathology.<sup>34</sup> These lesions are reported in patients between 16 and 80 years and are usually large lesions measuring over 7 cm.<sup>36</sup> They cause obstructive and irritative urinary symptoms due to their large size. The serum PSA level is often elevated in prostate cystadenoma while always normal in SV cystadenoma. Histological examination shows cysts lined by cuboidal cells without atypia in the background hypocellular stroma.<sup>34</sup> Immunohistochemical staining will be positive for PSA and prostate-specific acid phosphatase in prostate cystadenoma while they are negative in SV cystadenoma. Imaging helps in determining the epicenter of lesion (prostate or SV). Apart from the difference in the epicenter of the lesion, the imaging characteristics of both prostatic and SV cystadenomas are similar and are seen as large well-encapsulated multi-locular cystic masses that may have minimal solid areas (**Fig. 18** and **19**).<sup>56</sup> The cyst contents can range from simple fluid, to non-simple hemorrhagic or proteinaceous fluid, and imaging can show fluid-level levels. Enhancement of the septa and solid components may be observed. Surgical resection of the lesion is curative.

### Conclusion

Imaging diagnosis and differential diagnostic considerations for Non-malignant prostatic and SV lesions are broad. Along with the imaging findings, we must consider the clinical context, past medical history, treatment history, current symptoms, age of the patient, clinical examination findings, and serum PSA level to provide an accurate diagnosis and logical differential diagnosis. Knowledge of these conditions can help us identify or suspect entities that may mimic clinically significant prostate cancer on mpMRI in the appropriate clinical setting.

### Funding

None.

### Conflict of Interest

None declared.

### Acknowledgement

We sincerely acknowledge Departments of Urology and Infectious disease and the Uro-Oncology multi-disciplinary team (MDT) of Christian Medical College Vellore, India.

### References

- Borofsky S, George AK, Gaur S, et al. What are we missing? false-negative cancers at multiparametric MR imaging of the prostate. *Radiology* 2018;286(01):186–195
- Fütterer JJ, Briganti A, De Vissschere P, et al. Can clinically significant prostate cancer be detected with multiparametric magnetic resonance imaging? A systematic review of the literature. *Eur Urol* 2015;68(06):1045–1053
- Panebianco V, Giganti F, Kitzing YX, et al. An update of pitfalls in prostate mpMRI: a practical approach through the lens of PI-RADS v. 2 guidelines. *Insights Imaging* 2018;9(01):87–101
- Rosenkrantz AB, Taneja SS. Radiologist, be aware: ten pitfalls that confound the interpretation of multiparametric prostate MRI. *AJR Am J Roentgenol* 2014;202(01):109–120
- Han EA, Nandalur KR, Morgan MA, et al. MRI of benign prostatic hyperplasia: important pre- and posttherapeutic considerations. *Radiographics* 2023;43(05):e220096
- Turkbey B, Rosenkrantz AB, Haider MA, et al. Prostate imaging reporting and data system version 2.1: 2019 update of prostate imaging reporting and data system version 2. *Eur Urol* 2019 Sep;76(03):340–351
- Banner MP. Imaging of benign prostatic hyperplasia. *Semin Roentgenol* 1999;34(04):313–324
- Diaz TA, Benson B, Clinkenbeard A, Long JR, Kawashima A, Yano M. MRI evaluation of patients before and after interventions for benign prostatic hyperplasia: an update. *AJR Am J Roentgenol* 2022;218(01):88–99
- Wasserman NF, Spilseth B, Golzarian J, Metzger CJ. Use of MRI for Lobar classification of benign prostatic hyperplasia: potential phenotypic biomarkers for research on treatment strategies. *AJR Am J Roentgenol* 2015;205(03):564–571
- Wasserman NF. Benign prostatic hyperplasia: a review and ultrasound classification. *Radiol Clin North Am* 2006;44(05):689–710, viii
- Cheah PY, Liong ML, Yuen KH, et al. Chronic prostatitis: symptom survey with follow-up clinical evaluation. *Urology* 2003;61(01):60–64
- Krieger JN, Nyberg L Jr, Nickel JC. NIH consensus definition and classification of prostatitis. *JAMA* 1999;282(03):236–237
- Krieger JN, Dobrindt U, Riley DE, Oswald E. Acute Escherichia coli prostatitis in previously healthy young men: bacterial virulence factors, antimicrobial resistance, and clinical outcomes. *Urology* 2011;77(06):1420–1425
- Roberts RO, Lieber MM, Rhodes T, Girman CJ, Bostwick DG, Jacobsen SJ. Prevalence of a physician-assigned diagnosis of prostatitis: the Olmsted County Study of Urinary Symptoms and Health Status Among Men. *Urology* 1998;51(04):578–584
- Etienne M, Chavanet P, Sibert L, et al. Acute bacterial prostatitis: heterogeneity in diagnostic criteria and management. Retrospective multicentric analysis of 371 patients diagnosed with acute prostatitis. *BMC Infect Dis* 2008;8:12
- Shigehara K, Miyagi T, Nakashima T, Shimamura M. Acute bacterial prostatitis after transrectal prostate needle biopsy: clinical analysis. *J Infect Chemother* 2008;14(01):40–43

- 17 Shakur A, Hames K, O'Shea A, Harisinghani MG. Prostatitis: imaging appearances and diagnostic considerations. *Clin Radiol* 2021;76(06):416–426
- 18 Ha US, Kim ME, Kim CS, et al. Acute bacterial prostatitis in Korea: clinical outcome, including symptoms, management, microbiology and course of disease. *Int J Antimicrob Agents* 2008;31(Suppl 1):S96–S101
- 19 Inflammatory and Pain Conditions of the Male Genitourinary Tract: Prostatitis and Related Pain Conditions, Orchitis, and Epididymitis - ClinicalKey [Internet]. [cited 2023 Dec 11]. Accessed January 17, 2023 at: <https://www.clinicalkey.com#!/content/book/3-s2.0-B9780323546423000562?scrollTo=%23h10000225>
- 20 Haaga JR, Dogra VS, Forsting M, Gilkeson RC, Ha HK, and Sundaram M, eds. Mosby Elsevier; 2008
- 21 Shukla P, Gulwani HV, Kaur S. Granulomatous prostatitis: clinical and histomorphologic survey of the disease in a tertiary care hospital. *Prostate Int* 2017;5(01):29–34
- 22 Naik KS, Carey BM. The transrectal ultrasound and MRI appearances of granulomatous prostatitis and its differentiation from carcinoma. *Clin Radiol* 1999;54(03):173–175
- 23 Bour L, Schull A, Delongchamps NB, et al. Multiparametric MRI features of granulomatous prostatitis and tubercular prostate abscess. *Diagn Interv Imaging* 2013;94(01):84–90
- 24 Nghiem HT, Kellman GM, Sandberg SA, Craig BM. Cystic lesions of the prostate. *Radiographics* 1990;10(04):635–650
- 25 Shebel HM, Farg HM, Kolokythas O, El-Diasty T. Cysts of the lower male genitourinary tract: embryologic and anatomic considerations and differential diagnosis. *Radiographics* 2013;33(04):1125–1143
- 26 Curran S, Akin O, Agildere AM, Zhang J, Hricak H, Rademaker J. Endorectal MRI of prostatic and periprostatic cystic lesions and their mimics. *AJR Am J Roentgenol* 2007;188(05):1373–1379
- 27 Trivedi J, Sutherland T, Page M. Incidental findings in and around the prostate on prostate MRI: a pictorial review. *Insights Imaging* 2021;12(01):37
- 28 Nakamura Y, Shida D, Shibayama T, et al. Giant multilocular prostatic cystadenoma. *World J Surg Oncol* 2019;17(01):42
- 29 McDermott VG, Meakem TJ III, Stolpen AH, Schnall MD. Prostatic and periprostatic cysts: findings on MR imaging. *AJR Am J Roentgenol* 1995;164(01):123–127
- 30 Takahashi H, Potretzke TA, Kawashima A, Cheville JC, Masuoka S, Kim B. Imaging of the Bulbourethral (Cowper) gland: abnormalities and differential diagnosis. *Radiographics* 2022;42(07):2037–2053
- 31 Surana S, Elshazly M, Allam A, Jayappa S, AlRefai D. A case of giant Cowper's gland syringocele in an adult male patient. *Case Rep Urol* 2015;2015:682042
- 32 Wagemans MEHM, Tsachouridis G, Kuijper CF, de Mooij KL, Klijn AJ, de Jong TPVM. Cowper's syringocele in the pediatric population: a retrospective study of 122 patients. *J Pediatr Urol* 2019;15(05):546–551
- 33 Melquist J, Sharma V, Sciuolo D, McCaffrey H, Ali Khan S. Current diagnosis and management of syringocele: a review. *Int Braz J Urol* 2010;36:3–9
- 34 Moch H, Humphrey PA, Ulbright TM, Reuter V. WHO Classification of Tumours of the Urinary System and Male Genital Organs. Lyon, France: International Agency for Research on Cancer; 2016
- 35 Grignon DJ. Unusual subtypes of prostate cancer. *Mod Pathol* 2004;17(03):316–327
- 36 Marcal LP, Surabhi VR, Ramani NS, Katabathina VS, Paspulati RM, Prasad SR. Mesenchymal neoplasms of the prostate and seminal vesicles: spectrum of disease with radiologic-pathologic correlation. *Radiographics* 2022;42(02):417–432
- 37 Johnson MH, Carter HB. Stromal tumor of uncertain malignant potential (STUMP) with PSA >500 ng/ml: a case report. *Urol Case Rep* 2015;3(05):175–177
- 38 Hansel DE, Herawi M, Montgomery E, Epstein JI. Spindle cell lesions of the adult prostate | *Modern Pathology* [Internet]. Accessed January 17, 2023 at: <https://www.nature.com/articles/3800676>
- 39 Virarkar M, de Castro Faria S, Patnana M, Zhang M, Sagebiel T. Leiomyoma of the prostate: case report and review of the literature. *Clin Genitourin Cancer* 2018;16(04):e771–e776
- 40 Zhang Y, Zhao J, Xu P, Qi Q. Multiple schwannoma of the seminal vesicle: a case report. *Medicine (Baltimore)* 2020;99(33):e21603
- 41 Rha SE, Byun JY, Jung SE, Chun HJ, Lee HG, Lee JM. Neurogenic tumors in the abdomen: tumor types and imaging characteristics. *Radiographics* 2003;23(01):29–43
- 42 Seminal vesicle schwannoma presenting with left hydroureteronephrosis - PMC [Internet]. [cited 2023 Dec 11]. Accessed January 17, 2023 at: <https://www.ncbi.nlm.nih.gov/pmc/articles/PMC4216547/>
- 43 Solitary Fibrous Tumor of the Prostate A Case Report and Literature Review - PMC [Internet]. [cited 2023 Dec 11]. Accessed January 17, 2023 at: <https://www.ncbi.nlm.nih.gov/pmc/articles/PMC8621876/>
- 44 Herawi M, Epstein JI. Solitary fibrous tumor on needle biopsy and transurethral resection of the prostate: a clinicopathologic study of 13 cases. *Am J Surg Pathol* 2007;31(06):870–876
- 45 Ronchi A, La Mantia E, Gigantino V, et al. A rare case of malignant solitary fibrous tumor in prostate with review of the literature. *Diagn Pathol* 2017;12(01):50
- 46 Tanaka Y, Nakamoto A, Inada Y, Narumi Y, Hirose Y, Azuma H. A case of malignant solitary fibrous tumor of the prostatic urethra. *BJR Case Rep* 2018;4(04):20180034
- 47 McKenney JK. Mesenchymal tumors of the prostate. *Mod Pathol* 2018;31(S1):S133–S142
- 48 Pernick N. Adrenal gland and paraganglia. In: Yang XJ, Zhou M, eds. *Practical Genitourinary Pathology*. Cham, Switzerland: Springer; 2021:273–287
- 49 Padilla-Fernández B, Antúnez-Plaza P, Lorenzo-Gómez MF, Rodríguez-González M, Martín-Rodríguez A, Silva-Abuín JM. Paraganglioma of prostatic origin. *Clin Med Insights Case Rep* 2012; 5:69–75
- 50 Halat S, Eble JN, Grignon DJ, et al. Ectopic prostatic tissue: histogenesis and histopathological characteristics. *Histopathology* 2011;58(05):750–758
- 51 Yeager TS, Stroh BC, Youssef RE, Michaels PJ. Ectopic prostatic tissue involving the omentum and presenting with intussusception and small intestinal obstruction: a report of a rare case with a review of the literature. *Human Pathology Reports* 2022;30:300679
- 52 Dai S, Huang X, Mao W. A novel submucosa nodule of the rectum: A case of the ectopic prostatic tissue outside the urinary tract. *Pak J Med Sci* 2013;29(06):1453–1455
- 53 Roy C, Guth S, Gasser B, et al. Benign hyperplasia in ectopic prostatic tissue: a rare cause of pelvic mass. *Eur Radiol* 1997;7(01):35–37
- 54 Fulton RS, Rouse RV, Ranheim EA. Ectopic prostate: case report of a presacral mass presenting with obstructive symptoms. *Arch Pathol Lab Med* 2001;125(02):286–288
- 55 Vogel U, Negri G, Bültmann B. Ectopic prostatic tissue in the spleen. *Virchows Arch* 1996;427(05):543–545
- 56 Han C, Zhu L, Liu X, Ma S, Liu Y, Wang X. Differential diagnosis of uncommon prostate diseases: combining mpMRI and clinical information. *Insights Imaging* 2021;12(01):79